Received: 8 October 2022 | Revised: 18 November 2022 | Accepted: 21 November 2022

DOI: 10.1002/pro.4521

FULL-LENGTH PAPER

THE PROTEIN SOCIETY WILEY

Fused in sarcoma undergoes cold denaturation: Implications for phase separation

Sara S. Félix[1,2,3] | **Douglas V. Laurents**[3] | **Javier Oroz**[3] | **Eurico J. Cabrita**[1,2]

[1]UCIBIO, Department of Chemistry, NOVA School of Science and Technology, Universidade NOVA de Lisboa, Caparica, Portugal

[2]Associate Laboratory i4HB – Institute for Health and Bioeconomy, NOVA School of Science and Technology, Universidade NOVA de Lisboa, Caparica, Portugal

[3]Instituto de Química Física Rocasolano (IQFR), CSIC, Madrid, Spain

Correspondence
Javier Oroz, Instituto de Química Física Rocasolano (IQFR), CSIC, Madrid, E-28006, Spain.
Email: joroz@iqfr.csic.es

Eurico J. Cabrita, UCIBIO, Department of Chemistry, NOVA School of Science and Technology, Universidade NOVA de Lisboa, 2829-516, Caparica, Portugal.
Email: ejc@fct.unl.pt

Funding information
Fundação para a Ciência e a Tecnologia, Grant/Award Numbers: LA/P/0140/2020 PD/BD/148028/2019, ROTEIRO/0031/2013-PINFRA/22161/2016, UIDP/04378/2020, UIDB/04378/2020; Fundación BBVA, Grant/Award Number: BBM_TRA_0203; Ministerio de Ciencia e Innovación, Grant/Award Numbers: MCIN/AEI/10.13039/501100011033, PID-2019-109276RA-I00, PID-2019-109306RB-I00, RYC2018-026042-I

Review Editor: Aitziber L. Cortajarena

Abstract

The mediation of liquid–liquid phase separation (LLPS) for fused in sarcoma (FUS) protein is generally attributed to the low-complexity, disordered domains and is enhanced at low temperature. The role of FUS folded domains on the LLPS process remains relatively unknown since most studies are mainly based on fragmented FUS domains. Here, we investigate the effect of metabolites on full-length (FL) FUS LLPS using turbidity assays and differential interference contrast (DIC) microscopy, and explore the behavior of the folded domains by nuclear magnetic resonance (NMR) spectroscopy. FL FUS LLPS is maximal at low concentrations of glucose and glutamate, moderate concentrations of NaCl, Zn^{2+}, and Ca^{2+} and at the isoelectric pH. The FUS RNA recognition motif (RRM) and zinc-finger (ZnF) domains are found to undergo cold denaturation above 0°C at a temperature that is determined by the conformational stability of the ZnF domain. Cold unfolding exposes buried nonpolar residues that can participate in LLPS-promoting hydrophobic interactions. Therefore, these findings constitute the first evidence that FUS globular domains may have an active role in LLPS under cold stress conditions and in the assembly of stress granules, providing further insight into the environmental regulation of LLPS.

KEYWORDS

cold denaturation, cold stress, fused in sarcoma (FUS), liquid–liquid phase separation (LLPS), nuclear magnetic resonance (NMR)

1 | INTRODUCTION

Liquid–liquid phase separation (LLPS) of proteins is a fundamental biological mechanism that gives rise to microdroplets in cells (Banani et al., 2017; Brangwynne, 2013; Brangwynne et al., 2009; Elbaum-Garfinkle et al., 2015). These microdroplets, which are also called membraneless organelles or biomolecular condensates, are typically comprised of proteins and RNA and have been shown to behave as fluids with liquid-like properties (Buchan & Parker, 2009; Protter & Parker, 2016).

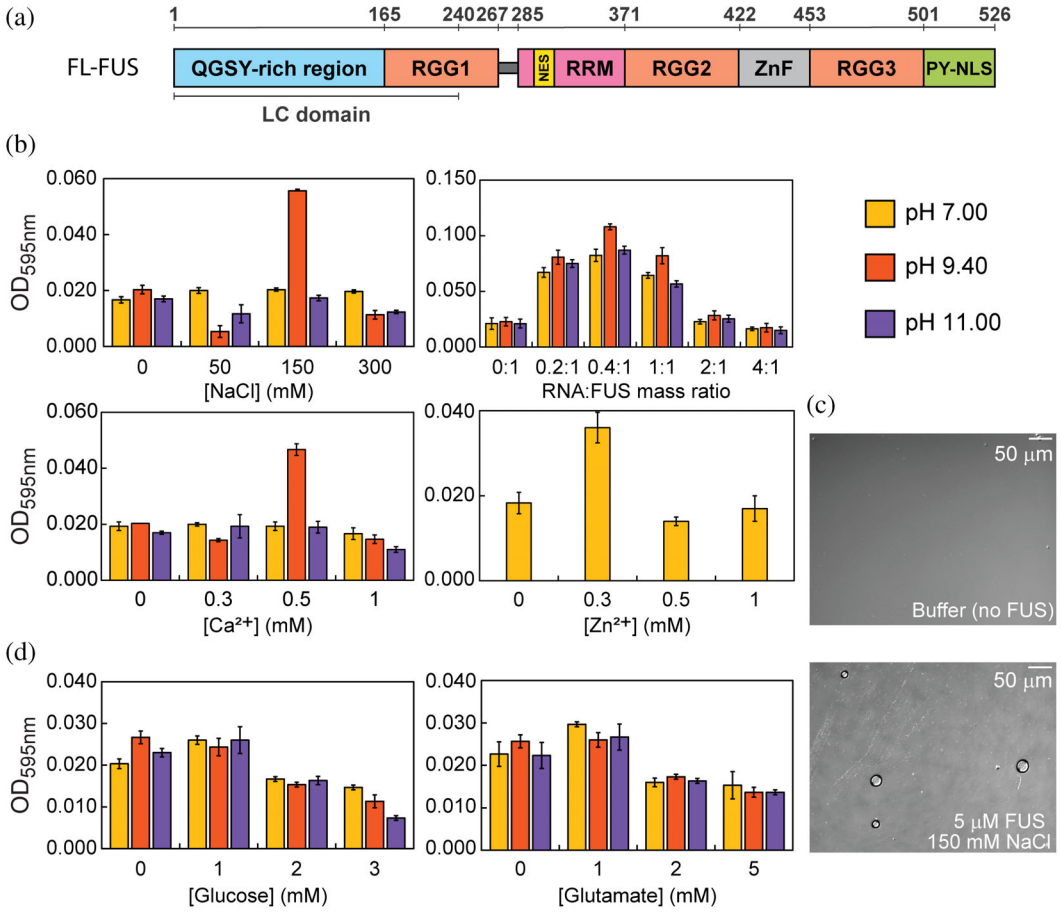

FIGURE 1 FL FUS phase separation is highly sensitive to the sample conditions. (a) FL FUS domain architecture. (b) Liquid–liquid phase separation (LLPS) of 5 μM FL FUS increases in the presence of specific concentration of NaCl (150 mM), RNA:FUS mass ratio (0.4:1), Zn^{2+} (0.3 mM), and Ca^{2+} (0.5 mM). This promotion of LLPS is not proportional to metabolite concentration, indicating the tight regulation of the phase separation of FUS. Overall, the phase separation is maximized when the pH = pI of FUS. Data are represented as triplicate mean ± SD. (c) DIC microscopy images of 5 μM FUS in 150 mM NaCl show LLPS droplets. (d) LLPS of 5 μM FL FUS decreases in the presence of stabilizing metabolites (glucose and glutamate). Color code in (b) is maintained in (d). DIC, differential interference contrast; FL FUS, full-length fused in sarcoma.

Recent research has shown that biomolecular condensates govern several biochemical processes, ranging from nucleic acid processing to age-related neurodegeneration (Kiwatkowsi et al., 2009; Li et al., 2013; Sun & Chakrabartty, 2017). Stress granules are an important class of biomolecular condensates. They assemble from pools of untranslated mRNA, RNA-binding proteins (RBPs) and factors involved in translational repression and mRNA decay, during adverse cellular conditions. Found in the cytoplasm, stress granules regulate RNA metabolism, stabilize translation preinitiation complexes, and modulate signaling pathways in response to stress stimuli (Buchan, 2014; Courchaine et al., 2016; Jain et al., 2016).

Fused in sarcoma (FUS) is a complex RBP that shuttles between the nucleus and the cytoplasm, where it may be sequestered into stress granules (Bentmann et al., 2012; Bosco et al., 2010; Gal et al., 2011). FUS is involved in the transcriptional regulation of cells (Chen et al., 2019) and its broad array of functions arises from its multidomain character. FUS contains an N-terminal low complexity (LC) domain that is enriched with glutamine, glycine, serine, and tyrosine (QGSY) residues, known to have an important role on protein self-association through the mediation of LLPS (Figure 1a) (Burke et al., 2015; Murakami et al., 2015). In addition, the protein contains a nuclear export signal (NES) and a proline-tyrosine nuclear localization signal (PY-NLS), involved in the nuclear-cytoplasmatic shuttling. Mediation of protein-nucleic acid interactions is governed by the three arginine-glycine–glycine (RGG) boxes, by the structured RNA recognition motif (RRM) and the cysteine$_2$-cysteine$_2$ zinc-finger (ZnF) domain (Deng et al., 2014; Loughlin et al., 2019; Yang et al., 2010). Apart from the RRM and ZnF motifs, the remaining domains are predicted to be highly disordered (Rogelj et al., 2012).

FUS is able to undergo LLPS both *in vivo* and *in vitro*, self-assembling into liquid-like phases at concentrations in the low micromolar range (Burke et al., 2015; Patel et al., 2015; Wang et al., 2018). FUS condensates are highly dynamic structures, displaying constant exchange of components with the cytoplasm and rapid internal rearrangement (Patel et al., 2015). While usually disordered, the FUS N-terminal region forms highly ordered amyloid fibrils that might be disease relevant (Murray et al., 2017). Since the cell uses dynamic liquid compartments to perform physiological relevant functions, there are mechanisms that prevent thermodynamically driven amyloidogenesis. Hence, FUS-related diseases often have a late onset, when the protein control machineries start to degenerate (Patel et al., 2015; Shin & Brangwynne, 2017). Aberrant aggregated forms of FUS are a major component of the pathological inclusions found in 5% of all forms of amyotrophic lateral sclerosis (ALS) and in 8% of all cases of frontotemporal lobar degeneration (FTLD) (Buchan & Parker, 2009; Yang et al., 2010).

FUS plays an imperative role in cellular stress response. Cells exposed to environmental stress, such as oxidative stress, hypoxia, viral infections, or osmotic stress, actively promote cytoplasmatic FUS stress granule formation (Bentmann et al., 2012; Bosco et al., 2010; Dormann et al., 2010). Interestingly, FUS phase separation has been shown to be highly enhanced at low temperature, suggesting that cold stress can also induce the stress granule assembly (Burke et al., 2015; Yoshizawa et al., 2018). In fact, cold stress has been identified as a trigger for stress granule assembly in yeast and mammals, acting as a protective mechanism against cell death during hypothermia, which suggest that FUS might have an active role in cold shock response (Al-Fageeh & Smales, 2006; Hofmann et al., 2012). Indeed, 4.5 million deaths per year are attributed to cold temperature exposure (Zhao et al., 2021). How hypothermia affects the survival of cells and, in particular, how it affects LLPS and biocondensate formation is still unclear. Our study aims to shed light on this matter.

In recent years, there have been fundamental advances in the LLPS field; from protein sequence determinants to favorable molecular interactions (Dignon et al., 2018; Mitrea & Kriwacki, 2016; Wang et al., 2018). However, there is still a need to investigate the specific triggers and determinants that lead to LLPS and eventually to the transition to proteinaceous deposits (Sama et al., 2014). Since the LLPS process relies on the establishment of weak interaction networks, it is believed that different environmental conditions and stresses, and consequently different interactions, should influence FUS LLPS (Darling et al., 2018; Protter & Parker, 2016; Uversky et al., 2015). Most LLPS studies are based on FUS domains or constructs containing a few domains with the justification that low-complexity domains are often sufficient for phase separation (Burke et al., 2015; Molliex et al., 2015; Xiang et al., 2015). However, it has been observed that ordered proteins can undergo LLPS (Annunziata et al., 2003; Da Vela et al., 2016; Li et al., 2012). Studies of full-length (FL) FUS and the interplay between disordered and folded domains are still scarce, which is probably due to the elevated tendency for the FL FUS to stick to surfaces and to readily aggregate (Hamad et al., 2021; Patel et al., 2015). For this reason, the possible contributions of the well-structured RRM and ZnF domains of FUS to LLPS are poorly understood.

In this study, the LLPS of FL FUS is to detect possible synergies between the different disordered and folded domains. We use a novel sample preparation and handling protocol to minimize surface binding and aggregation. We seek to unravel the connection between cold stress and FUS phase separation and to assess the influence of diverse environmental conditions in the formation of FL FUS stress granules, using a combination of nuclear magnetic resonance (NMR) spectroscopy, differential interference contrast (DIC) microscopy, and turbidity assays.

Insights on the role of the environment on the LLPS mechanism can prove valuable in understanding the physiological and pathological conditions that trigger FL FUS stress granule assembly. Our results provide the first structural insight into the possible influence of cold stress on FUS protein and how phase separation could be regulated by cold stress conditions.

2 | RESULTS

2.1 | Charged metabolites and a net neutral charge enhance FUS phase separation

Charged metabolites are ubiquitous in cells, being crucial for almost all cellular processes. For this reason, the influence of inorganic salt ions (Na^+ and Cl^-), metal ions (Ca^{2+} and Zn^{2+}), and RNA in the FUS LLPS mechanism, was tested by turbidity assays, following the OD at 595 nm. Although turbidity assays of FL FUS have been previously reported, those experiments were generally done with FUS tagged with maltose-binding protein (MBP) in the presence of Tobacco etch virus (TEV) protease (Ahlers et al., 2021; Burke et al., 2015; Kaur et al., 2019). Since it was reported that FUS phase separation is highly sensitive to crowding and prone to unspecific interactions with proteins (Kang et al., 2019; Kaur

et al., 2019; Lin et al., 2015), it is possible that the presence of cleaved MBP tag and of TEV protease in the solution could affect the turbidity results and analyses. Therefore, we performed the LLPS turbidity assays with pure non-tagged, FL FUS (Figure 1a). It is important to note that our studies were performed with FL FUS under conditions where the ZnF domain is stabilized and folded (purified in the presence of supplemental Zn^{2+}). So, for the study of the effect of the Zn^{2+} cation on the LLPS process, the concentration of 0 mM Zn^{2+} in the turbidity assays does not take into account the Zn^{2+} complexed with the ZnF domain.

FL FUS phase separation displayed a high sensitivity to the nature and concentration of each metabolite in a pH-dependent manner (Figure 1b). LLPS was observed to be maximal when the protein's overall net charge is 0, at pH 9.40. Among all tested metabolites, FUS LLPS was notably promoted by 150 mM NaCl. However, increasing NaCl concentration resulted in inhibition of phase separation. Similar results have been previously observed with MBP-FUS, where high salt concentration decreased LLPS (Burke et al., 2015). Nevertheless, the phase separation behavior of FL FUS is different from that of the FUS LC region, where the LLPS increased with increasing NaCl concentration (Burke et al., 2015). This suggests that charge screening of FL FUS might be crucial for LLPS promotion, contrary to FUS LC. Efficient FUS phase separation with 150 mM NaCl was further confirmed by DIC imaging (Figure 1c).

The modulation of FUS phase separation by the divalent cations Zn^{2+} and Ca^{2+} is distinct from Na^{+}. Under stress conditions, the flux of divalent cations is correlated to distinct phase-separation behavior of proteins. Switch-like behavior has been observed in RNA droplets, whereas low and high concentrations of Mg^{2+} promote LLPS, intermediate concentration abrogates it (Onuchic et al., 2019). In other cases, divalent cations promote phase separation at higher concentration (Singh et al., 2020).

In the case of FL FUS, both Ca^{2+} and Zn^{2+} induced phase separation at concentrations about 300-fold lower compared to the tested monovalent ions. LLPS was promoted at intermediate concentration and inhibited at lower and higher concentration (Figure 1d). This reveals the role of direct binding of these divalent cations in the FUS LLPS process.

2.2 | Stabilizing metabolites hinder FUS LLPS

Glucose and glutamate are two of the most abundant metabolites found in cells, and both are stabilizing as they induce preferential hydration of proteins (Psychogios et al., 2011; Scimemi & Beato, 2009). This prompted us to investigate how these metabolites affect FUS LLPS.

Our results showed that in the presence of increasing glucose or glutamate concentrations, FUS phase separation was inhibited at all pH values studied (Figure 1d). By inducing preferential hydration, glucose and glutamate are capable of displacing water molecules from the protein surface leading to structural compaction and a reduction in the exposed protein surface area (Arakawa & Timasheff, 1982; Arakawa & Timasheff, 1984). The observed decrease of FUS phase separation by glucose and glutamate suggests that the FUS phase-promoting interacting sites may be covered or inaccessible.

2.3 | FUS RRM and ZnF domains undergo cold denaturation

To understand how cold shock could affect FUS phase separation, our first approach was to investigate the impact of cold stress on FUS structure by NMR spectroscopy. By the acquisition of ^{1}H-^{15}N TROSY-HSQC and ^{1}H-^{15}N HSQC spectra, we followed FL FUS structural changes induced by temperature, from physiological temperature (37°C) to mild hypothermia (35–25°C) and to severe hypothermia (15–5°C) in the absence of excess of $ZnCl_2$.

As the temperature decreased, the signals from the folded regions (corresponding to the RRM and ZnF domain) lost intensity and re-emerged in the disordered region of the spectrum, between 8 and 9 ppm (Figure 2a). This is especially clear in the 1D ^{1}H projection of the ^{1}H-^{15}N TROSY-HSQC spectra (Figure 2b) where, as the temperature lowers, the intensity of the proton signals in the unfolded region increases. Using assignments available in the BioMagResBank (BMRB) database (BMRB LC #26672 and RRM #34259), we could identify several isolated cross-peaks belonging to the LC and RRM domains from FUS. We analyzed the intensity of the LC domain and RRM cross-peaks as the temperature decreased (Figure 3a). While the LC domain cross-peaks disappeared at higher temperature (>30°C) due to chemical exchange, those belonging to the folded RRM domain disappeared at lower temperature (<15°C), indicating domain unfolding. When the sample was reheated to 37°C, the cross-peaks reverted to the initial position, showing that the process is reversible. These results showed that, in the absence of excess $ZnCl_2$, which renders an unstable ZnF motif, FUS folded domains undergo reversible cold denaturation.

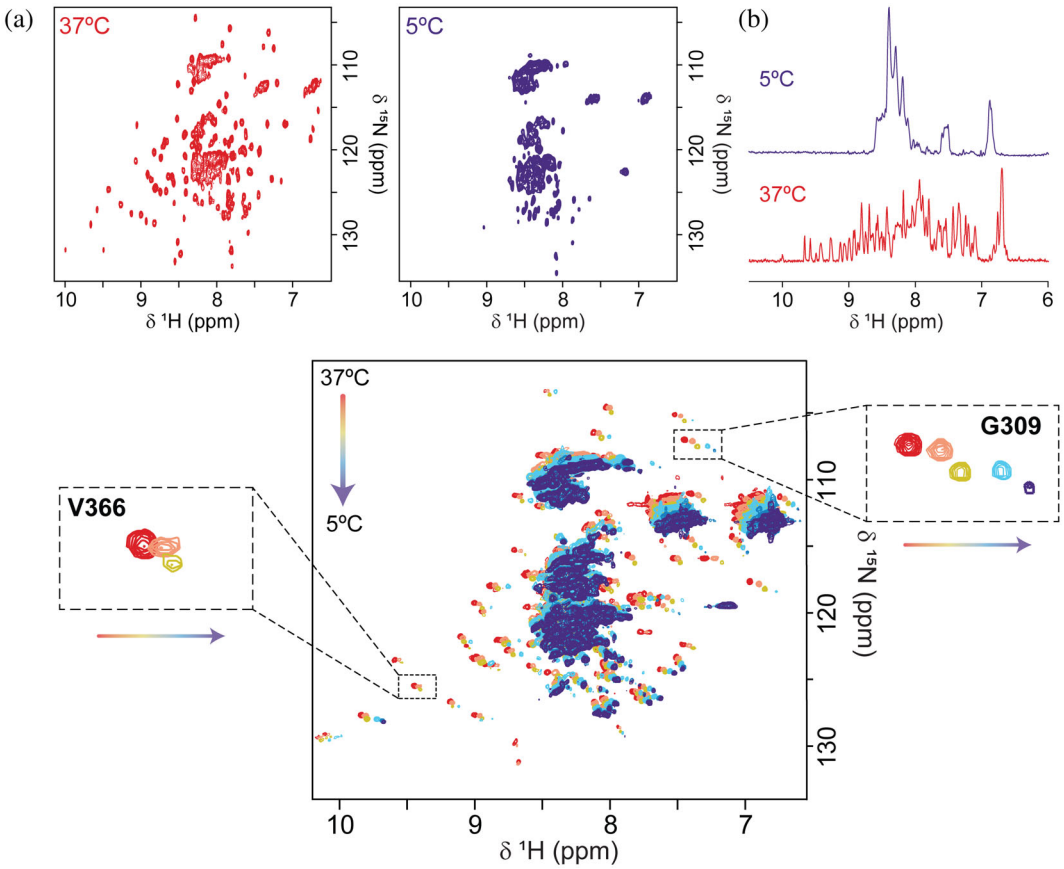

FIGURE 2 FUS globular domains undergo cold denaturation above 0°C in the absence of excess Zn^{2+}. (a) ^{1}H-^{15}N TROSY-HSQC spectra of 30 μM FL FUS from 37°C to 5°C revealing cold denaturation (37°C red, 30°C pink, 25°C yellow, 15°C light blue, and 5°C dark blue). Example of valine 366 from structured region of the RRM domain which disappears at low temperature opposed to glycine 309 from disordered coil region of the RRM. (b) ^{1}H projections of FUS ^{1}H-^{15}N TROSY-HSQC spectra at 37°C and 5°C showing the collapse of peak chemical shifts in the disordered region 8–9 ppm. FL FUS, full-length fused in sarcoma.

2.4 | Cold denaturation of FUS is independent of phase separation

To ensure that the changes in NMR signal intensity were not due to FL FUS phase separation, turbidity was checked at each temperature (Table S1) and peak analysis showed that ^{1}H linewidths remain almost unchanged at each temperature (Figure 3b). NMR signal linewidth would be expected to increase proportionally as phase separation occurred due to the higher viscosity of the sample (Burke et al., 2015). Hence, during the temperature variation experiment, the sample remained dispersed and the drop in intensity in the folded regions can be attributed to local unfolding as the temperature decreases.

Nevertheless, to corroborate that the spectral changes were a result of cold denaturation and not phase separation or a combination of both, the NMR experiments were also performed with FUS in the phase-separated state, and in the presence of 4% 1,6-hexanediol. This aliphatic alcohol has been showed to completely disrupt phase separation of FUS at 4% concentration (w/v) (Kroschwald et al., 2017). This experiment was used as a negative control, where FUS is completely dispersed in solution (Table S1). The same behavior was observed in the NMR spectra both in presence and in the absence of 4% 1,6-hexanediol, indicating that the spectral changes do not come from phase separation and can be attributed to cold denaturation (Figure 4). This was substantiated by NMR experiments of FL FUS in the phase-separated state that served as a positive control, which showed the complete loss of signal upon LLPS (Figure S1).

Inspired by the standard procedure to induce cold denaturation of proteins above the water freezing temperature using denaturing agents (Agashe & Udgaonkar, 1995; Privalov, 1990; Wong et al., 1996), urea was added to FUS samples and spectral changes over a temperature range were followed. Chaotropic agents such as urea are able to shift cold denaturation equilibrium towards higher temperatures in order to detect unfolded populations. In the presence of 750 mM urea, cold

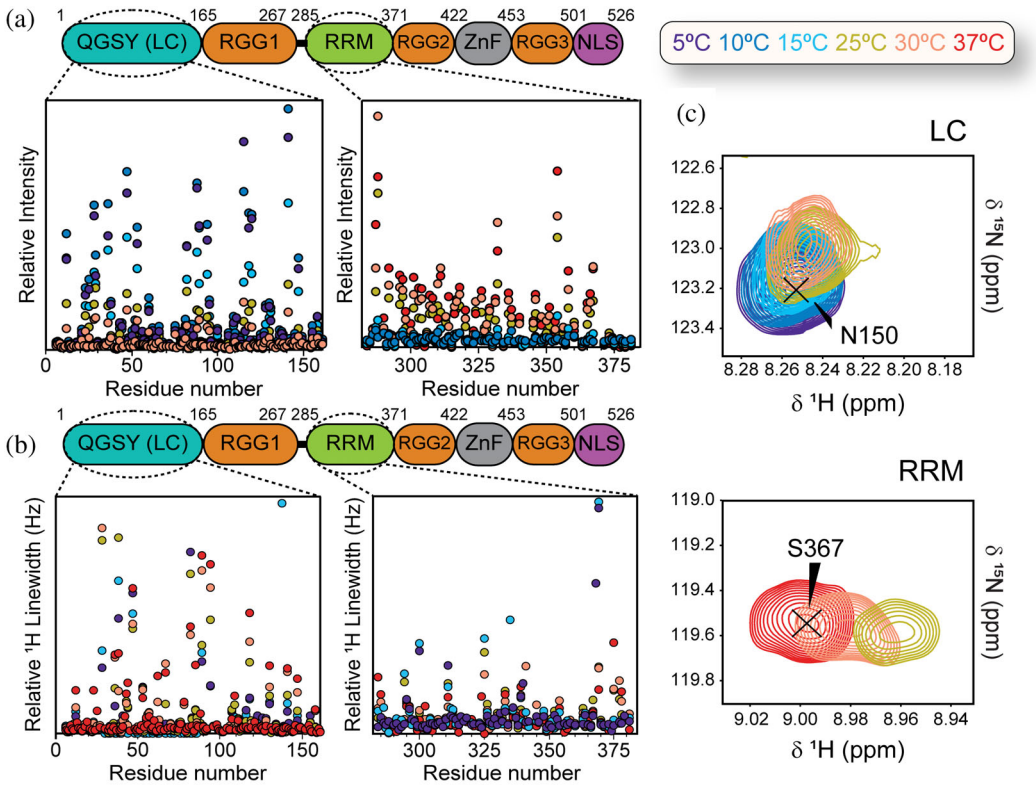

FIGURE 3 Analysis of the NMR cross-peaks from order vs disordered regions of FL FUS. (a) Intensity plots of the ^{1}H-^{15}N HSQC spectra at different temperatures (as indicated in the color code) from the LC and RRM domains of FUS. LC moiety peaks disappear at higher temperature due to chemical exchange, while RRM peaks fade out at low temperature, indicating domain unfolding. (b) Linewidth analysis of the ^{1}H-^{15}N HSQC spectra from the LC and RRM across the different temperatures, showing that in each domain the linewidth of the cross-peaks remains roughly unchanged. (c) Representative amino acid residues belonging to the LC and RRM domain. Intensity of the LC cross-peak decreases as the temperature increases, while the RRM cross-peak disappears at lower temperature. In both, the linewidth remains almost unaffected. FL FUS, full-length fused in sarcoma; LC, low complexity; NMR, nuclear magnetic resonance; RRM, RNA recognition motif.

denaturation of FL FUS is indeed detected at higher temperatures compared to in the absence of urea (Figure 5). This experiment thus provides additional evidence that folded domains of FUS are undergoing cold denaturation.

2.5 | The presence of Zn^{2+} partially protects FUS from cold denaturation

Remarkably, when 100 μM of $ZnCl_2$ was added to FUS, cold denaturation was not observed at the same degree when compared to samples without supplemental $ZnCl_2$ (Figure 6), as signals from the folded regions (corresponding to the RRM and ZnF domain) are still visible at 5°C. In the presence of added Zn^{2+}, FUS samples are overall more stable, which could be attributed to the native coordination of Zn^{2+} in the ZnF domain. Still, it was observed that several residues show chemical shift deviations or loss in intensity at lower temperature, indicating that even in the presence of Zn^{2+}, temperature is influencing the local environment of the protein. These results indicate that Zn^{2+} ions protect FUS from cold denaturation and might provide a direct link between zinc dyshomeostasis and ALS pathology.

A recent study of LLPS for various FUS domain constructs at one fixed temperature (25°C) and pH (6.0), reported that the ZnF domain is fully denatured when stripped of Zn^{2+} (Kang et al., 2019). ZnF domains bind tightly to Zn^{2+} typically with pM dissociation constants, and also to Co^{2+} and Ni^{2+} with μM – nM K_Ds (Kluska et al., 2018). Considering that under our conditions, FL FUS's ZnF domain might have bound Zn^{2+} or Ni^{2+} during the protein production and purification processes, we sought to further confirm our findings by studying the ZnF domain alone as a polypeptide produced by solid phase chemical synthesis. The results, which are described in detail in Figure S2, corroborate the following results of Kang et al. (2019): (1) Without added Zn^{2+}, the ZnF domain is fully unfolded over a wide range of

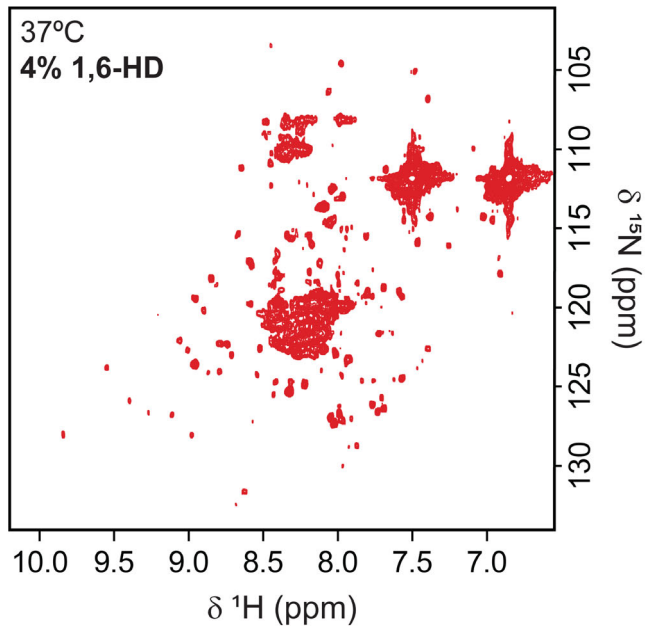

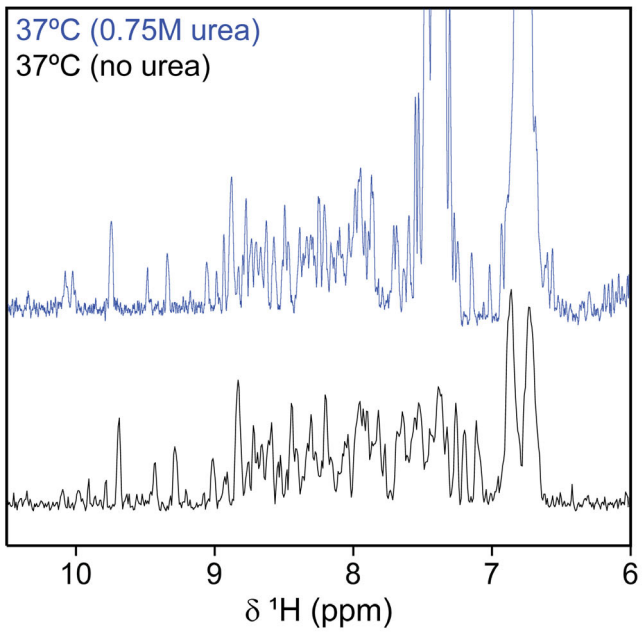

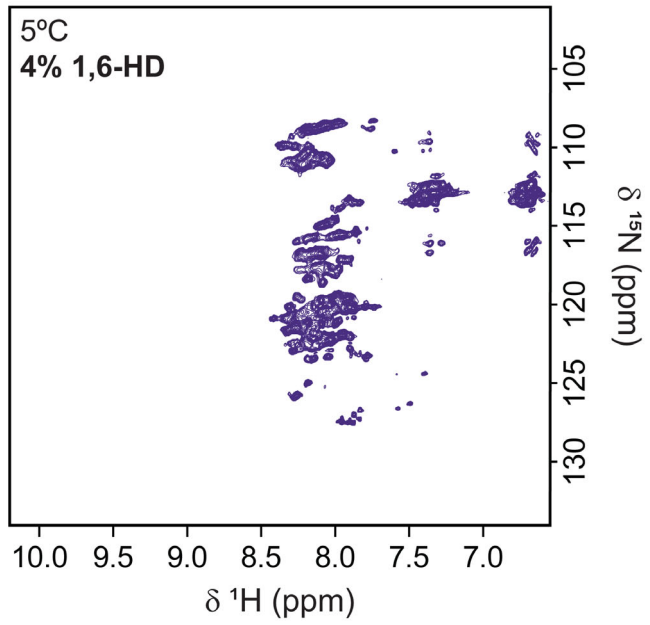

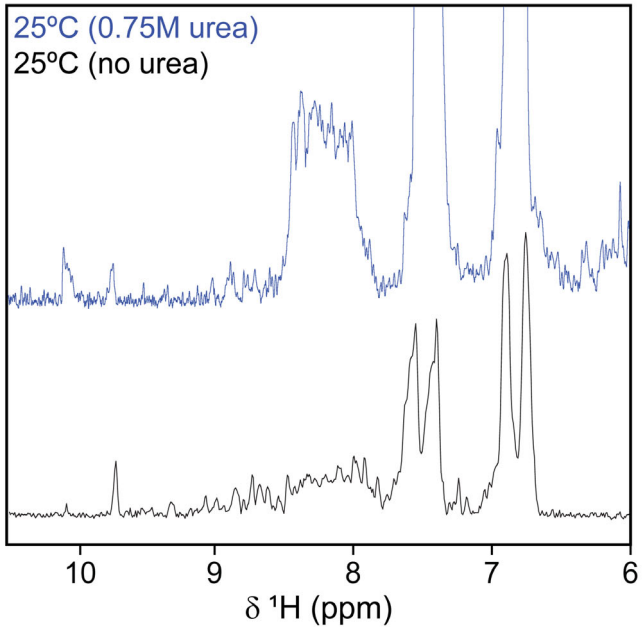

FIGURE 4 Cold denaturation of FUS is still detected in the presence of liquid-phase inhibitor 1,6-hexanediol. Negative control ^{1}H-^{15}N HSQC spectrum of 30 μM FL FUS in the presence of 4% 1,6-hexanediol (1,6-HD), indicating that the spectral changes are not due to phase separation. FL FUS, full-length fused in sarcoma.

FIGURE 5 Urea shifts cold denaturation temperature equilibrium towards higher temperatures. ^{1}H NMR spectrum reveals that 30 μM FL FUS in the presence of 0.75 mM urea undergoes cold denaturation at higher temperature compared to without urea. In the presence of urea, there is a large increase of intensity in the region 8–9 ppm at 25°C (lower panel) which indicates substantial protein unfolding, whereas no significant changes are seen at 37°C (upper panel). Without urea, the unfolding only starts at ≤15°C. NMR, nuclear magnetic resonance; FL FUS, full-length fused in sarcoma.

temperatures (0–37°C), (2) the ZnF domain folds within minutes upon adding an excess of $ZnCl_2$, and (3) With Zn^{2+} bound, the ZnF domain has a modest conformational stability as all the ^{1}HN groups exchange within minutes upon dissolving in buffer prepared with 100% D_2O. In addition, by monitoring the intensity of Lys451 methylene ^{1}H signals, which are shifted upfield due to ring current interactions with Trp440 when the ZnF domain is folded (see Loughlin et al., 2019 and BMRB 34258), cold denaturation was confirmed (Figure S2). Since these ^{1}H Lys methylene resonances are not subject to solvent exchange broadening (in contrast to ^{1}HN

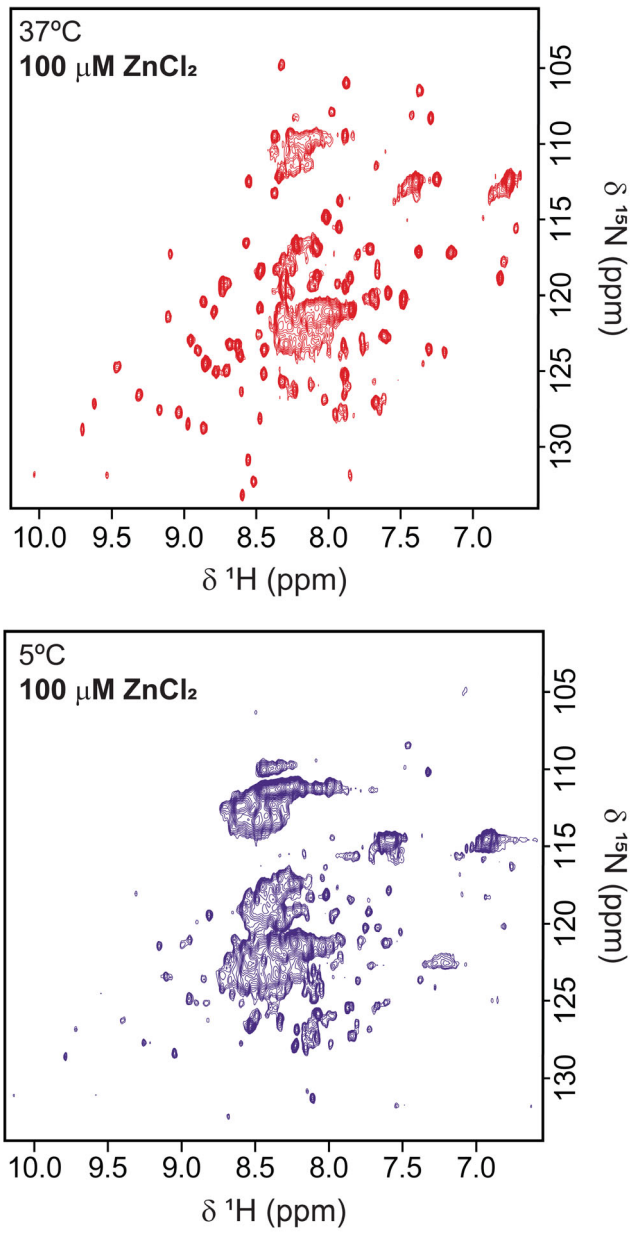

FIGURE 6 In the presence of supplemental $ZnCl_2$ cold denaturation of FL FUS is not complete above 0°C. ^{1}H-^{15}N TROSY-HSQC spectra of 30 μM FL FUS in the presence of 100 μM $ZnCl_2$, at different temperatures, revealing that cold denaturation is not complete at 5°C (lower panel) opposed to in the absence of excess $ZnCl_2$. This suggests that proper coordination of ZnF domain is pivotal for the process to occur above 0°C. FL FUS, full-length fused in sarcoma.

signals), these results are an important additional confirmation of FUS ZnF cold denaturation.

Taken together, these results show that the RRM and ZnF domains of FUS undergo gradual cold denaturation upon cooling towards 0°C, at physiological pH. In addition, we found that the stability of the ZnF largely influences this process.

3 | DISCUSSION

3.1 | Cold denaturation in protein stability and function

Cold denaturation is a universal characteristic of proteins as their folding thermodynamics are governed by a modest conformational stability (ΔG) (Pace & Hermans, 1975) and large and highly temperature-dependent enthalpy (ΔH) and entropy (ΔS). The heat capacity change for folding (ΔC_P) determines the temperature dependence of ΔH and ΔS and this parameter scales, in general, with the size and hydrophobicity of proteins (Myers et al., 1995). For this reason, protein cold denaturation has been observed in only a handful of small proteins such as Barstar (Agashe & Udgaonkar, 1995) UBA(2) (Scheper & Hoozemans, 2009), L9 protein mutants (Shan et al., 2010), yeast Yfh1 protein (Martin et al., 2008; Sanfelice et al., 2015), HIV-1 protease (Rösner et al., 2017), *Escherichia coli* IscU (Yan et al., 2018) and the bacterial cold shock protein BcCsp (Szyperski et al., 2006). Despite having different structures and functions, it has been pointed out that BcCsp and UBA(2) have low per-residue ΔH and high per-residue ΔC_P values, and we note that this trend also holds for Barstar and the FUS ZnF.

A recent study has demonstrated that unfolding of the FUS RRM is a key driver of condensate aging, prevented by HspB8 chaperoning (Boczek et al., 2021). The authors show that after FUS condensation, multiple RRM intra- and inter-molecular contacts increased inside the condensates, suggesting RRM structural changes upon LLPS. In our study, we establish that structural changes of the RRM indeed occur via a phase-separation mediator, cold shock, which leads to the cold denaturation of the domain. This phenomenon could also help explain why FUS condensate aging occurs over time. Persistent cold shock may incite the RRM domain to remain unfolded for extended times which in turn drives condensate degeneration.

In this study, we reveal that FL FUS undergoes cold unfolding and that the stability of the ZnF domain, which is determined by the presence of Zn^{2+} cations, influences the overall process. Cold denaturation is observed when FL FUS contains an unstable ZnF (purified and studied in the absence of excess Zn^{2+}).

We observed a dual effect of Zn^{2+} cations. In the presence of FUS with stable ZnF-Zn^{2+}, additional Zn^{2+} promotes phase separation at intermediate concentrations, likely due to electrostatic screening. However, when FUS has an unstable ZnF, supplemental Zn^{2+} stabilizes the ZnF and protects, to some extent, FUS from cold denaturation. Zinc ions probably act opposed to

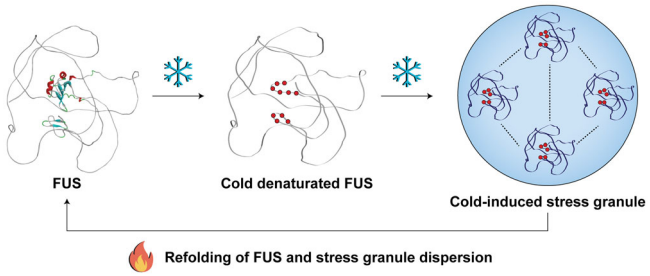

FIGURE 7 Schematic hypothesis of the implication of FUS cold denaturation on the formation of stress granules. In physiological conditions, FUS ordered domains are properly folded but upon cold stress, the domains undergo cold denaturation. This allows the exposure of buried hydrophobic residues (represented as red dots) that participate in LLPS-promoting hydrophobic interactions, leading to the assembly of stress granules. Upon temperature increase and reinstatement of physiological conditions, FUS ordered domains refold and cold-induced stress granules disassemble. FL FUS protein structure predicted by Alpha Fold (Jumper et al., 2021; Varadi et al., 2022). The α-helices and β-strands of the RRM and ZnF domains are colored in red and blue, respectively, and the intrinsically disordered domains are represented in gray. FL FUS, full-length fused in sarcoma; LLPS, liquid–liquid phase separation; RRM, RNA recognition motif.

urea, shifting cold denaturation equilibrium towards lower temperatures.

The observed role of Zn^{2+} in FUS cold denaturation mechanism might be intimately linked to the zinc homeostasis dysregulation that is associated with ALS pathology (Sirabella et al., 2018). In the absence of Zn^{2+}, Cu/Zn-superoxide dismutase 1 (SOD1) displays propensity to misfold and self-aggregate in toxic amyloid-like species which are found in 20% of ALS patients (Sirangelo & Iannuzzi, 2017). In the presence of unstable ZnF, FUS might likewise display a propensity to phase-separate due to the cold denaturation mechanism which could in turn trigger aggregation. But, when FUS contains a properly folded and stable ZnF, additional Zn^{2+} does not contribute to stability, but acts as modulator of phase separation.

In conclusion, we hypothesize that as a response to cold shock, FUS undergoes cold denaturation, which might expose otherwise buried hydrophobic residues, promoting LLPS, and consequently aggregation, via additional hydrophobic interactions (Figure 7). Furthermore, this process should be exacerbated in situations of zinc dysregulation.

FUS structural changes with temperature may provide a fast-acting cellular response to cold stress, allowing the rapid condensate assembly and dissolution mediated by the unfolding and refolding of the globular domains.

4 | MATERIALS AND METHODS

4.1 | Production of FL-FUS protein

Recombinant MBP-FUS construct was kindly gifted by Prof. Nicolas Fawzi (Addgene plasmid #98651) and was expressed in BL21 (DE3) *E. coli* cells. Non-labeled FUS were expressed in LB medium supplemented with 50 μg/ml kanamycin, while uniformly $^{13}C/^{15}N$-labeled FUS was expressed in M9 medium supplemented with 50 μg/ml kanamycin containing ^{13}C-glucose and ^{15}N ammonium chloride as the sole carbon and nitrogen source, respectively. Recombinant protein expression was induced at mid-exponential growth (OD_{600} 0.7–0.8) with 1 mM isopropyl-β-D-1-thiogalactoside (IPTG) for 8 h at 30°C. Cells pellets were resuspended in 50 mM Tris–HCl, 1 M NaCl, 10% glycerol, 1 M urea, 10 mM imidazole, 50 mM glycine, 2 mM β-mercaptoethanol, 2 mM benzamidine, 0.1 mM phenylmethylsulfonyl fluoride (PMSF) and EDTA-free complete mini protease inhibitor tablet (Roche), at pH 7.40, either in the absence or presence of 100 μM $ZnCl_2$. Cells were lysed through sonication and the lysate was cleared by centrifugation at 15,151 x *g* for 90 min.

All the purification and dialysis steps were performed in temperature-controlled rooms at 25°C, and all the tubes, buffers, and columns were pre-warmed to 30°C before use. This ensured that FUS remained soluble and inhibited unspecific binding to the laboratory materials and column resins.

Affinity purifications were performed on an AKTA Start chromatography system (Cytiva). The clarified lysate was loaded onto 2 x 5 ml HisTrap FF crude columns (Cytiva) and eluted with 150 mM imidazole. MBP-FUS-containing fractions were dialyzed overnight against 20 mM Tris–HCl, 500 mM NaCl, 1 M urea, 10% glycerol, 2 mM $MgSO_4$, 100 μM $ZnCl_2$, 2 mM β-mercaptoethanol, 2 mM benzamidine, 0.1 mM PMSF, and 0.03% NaN_3, at pH 7.40. Benzonase nuclease (Merck) was added to the sample, in a final concentration of 15 U/ml, to remove the nucleic acids bound to FUS. To remove the Benzonase, the dialyzed sample was purified using a 5 ml HisTrap HP column (Cytiva). The MBP tag was cleaved overnight using TEV protease (produced in house) in the aforementioned buffer lacking 2 mM $MgSO_4$. The cleaved product was applied to 2 x 5 ml HisTrap HP columns, where FUS eluted in the flow-through. The purified protein fractions were collected and stored at 30°C without further concentration. Before use, freshly prepared FUS was dialyzed against the desired buffer and subsequently concentrated using Vivaspin 15 Ultrafiltration units (Sartorius). Protein purity was confirmed by SDS-PAGE and ^{1}H-^{15}N TROSY/HSQC spectra. The $A_{260nm}/_{A280nm}$

values obtained for pure FUS-containing samples were between 0.60 and 0.70, indicating a nucleic acid-free protein.

4.2 | Phase separation assays

Assessment of FUS phase separation in different conditions and in the presence of metabolites was performed by turbidity assays. Experiments were carried out by monitoring the OD at 595 nm, using a Benchmark Microplate Reader (Bio-Rad).

All assays were executed with 5 μM of pure FL FUS in 20 mM Tris–HCl pH 7.00, 20 mM CAPS pH 9.40, and 20 mM CAPS pH 11.00. Exceptions were made when the pH influenced the solubility or stability of the studied metabolites. In particular, the turbidity of FUS solutions in the presence of $ZnCl_2$ was only measured at pH 7.00, since Zn^{2+} forms an insoluble hydroxide at pH 9.40 and 11.00.

In general, metabolites or RNA solutions in variable concentrations were added to a 96-flat-bottom-well clear microplate (Corning) to a final 100 μl reaction volume. Solutions were subsequently incubated for 60 min at 4°C without agitation. FUS was later added, incubated for additional 10 min and briefly mixed, before the turbidity assays. All measurements were made in triplicate.

4.3 | NMR spectroscopy

All NMR experiments were acquired in Bruker Avance III 600 MHz (^{1}H) and Neo 800 MHz (^{1}H) NMR spectrometers (Bruker BioSpin), equipped with cryogenic probes and Z-gradients. Chemical shifts were calibrated through indirect referencing using 50 μM sodium trimethylsilylpropanesulfonate (DSS) (Eurisotop) in all samples. All data were processed using Bruker TopSpin 4.0.6 software (Bruker BioSpin) and analyzed with CARA and PINT (Ahlner et al., 2013; Keller, 2004).

For the NMR studies, ^{13}C/^{15}N-labeled FUS samples were prepared in 90% H_2O/10% D_2O (Eurisotop) and transferred to 3 mm NMR tubes. Protein samples were prepared to a final concentration between 30 and 40 μM in 20 mM Tris–HCl, 100 mM NaCl, 5% glycerol, 2 mM β-mercaptoethanol, 0.03% NaN_3, at pH 7.00, with or without 100 μM $ZnCl_2$. To ensure that FUS was dispersed in these conditions, experiments were replicated in the presence of 4% 1,6-hexanediol (negative control). As a positive control, sample which contained 30 μM of phase-separated ^{15}N-labeled FUS (as measured by turbidity) was prepared as described in Data S1. Samples of FUS in the presence of urea were prepared by adding urea to the protein to a final concentration of 750 mM.

Temperature influence on the structure of dispersed FUS was followed by ^{1}H-^{15}N TROSY-HSQC and ^{1}H-^{15}N HSQC spectra, recorded at 37°C, 30°C, 25°C, 15°C, 10°C, and 5°C. The ^{1}H-^{15}N TROSY-HSQC spectra were acquired with 64 scans on a matrix with 2048 × 128 complex points, and a sweep width of 7812 Hz (centered at the water resonance frequency) × 2311 Hz (centered at 118 ppm), in the ^{1}H and ^{15}N dimensions, respectively. In turn, the ^{1}H-^{15}N HSQC spectra were acquired on an 800 MHz NMR spectrometer with 256 scans on a matrix with 2048 × 128 complex points, and a sweep width of 3758 Hz × 9445 Hz (centered at 116.5 ppm). 3D HNCO spectra were additionally recorded at different temperatures to confirm the proper transfer of the available assignments of the LC, RRM, and ZnF domains of FUS (BMRB codes #26672, #34259, and #34258, respectively) to our spectra. On the same sample, spectra were recorded from 5°C to 37°C to determine the reversibility of unfolding.

4.4 | DIC microscopy

DIC imaging was performed using a Zeiss Axio Imager D2 microscope equipped with Zeiss 10× and 40× Plan-Neofluar objectives and Zeiss DIC EC PN 10×/40× prism sliders. Samples of 5 μM FUS in 20 mM Tris–HCl, 150 mM NaCl and 2 mM β-mercaptoethanol at pH 7.40, were spotted onto glass slides, covered with coverslips and micrographed upright. Images were processed with ImageJ (Fiji) (Schindelin et al., 2012).

AUTHOR CONTRIBUTIONS

Sara S. Félix: Conceptualization (equal); formal analysis (equal); investigation (equal); methodology (lead); writing – original draft (lead); writing – review and editing (equal). **Douglas V. Laurents:** Conceptualization (equal); formal analysis (equal); investigation (equal); methodology (supporting); supervision (equal); writing – review and editing (supporting). **Javier Oroz:** Conceptualization (equal); formal analysis (equal); investigation (supporting); methodology (supporting); supervision (equal); writing – review and editing (supporting). **Eurico Cabrita:** Conceptualization (equal); formal analysis (equal); funding acquisition (lead); investigation (lead); methodology (supporting); project administration (lead); resources (lead); supervision (equal); writing – original draft (supporting); writing – review and editing (lead).

ACKNOWLEDGMENTS

The authors would also like to acknowledge Prof. Dr. Jaime Mota, Dra. Irina Franco for the technical assistance with the microscopic experiments, Philip O'Toole for the aid in protein production and Dr. Aldino Viegas and Dr. David Pantoja-Uceda for the support and valuable discussions regarding NMR spectroscopy. This work was supported by Fundação para a Ciência e a Tecnologia (FCT-Portugal) for funding UCIBIO project (UIDP/04378/2020 and UIDB/04378/2020) and Associate Laboratory Institute for Health and Bioeconomy – i4HB Project (LA/P/0140/2020). The authors also thank FCT-Portugal for the PhD grant attributed to SF (PD/BD/148028/2019) under the PTNMRPhD Program. JO is a recipient of a Leonardo Grant from the Spanish BBVA Foundation (BBM_TRA_0203) and a Ramón y Cajal Grant (RYC2018-026042-I funded by MCIN/AEI/10.13039/501100011033 and by "ESF Investing in your future.") JO and DVL are supported by the Spanish Grants PID-2019-109276RA-I00 and PID-2019-109306RB-I00, respectively, both funded by MCIN/AEI/10.13039/501100011033. The NMR spectrometers are part of the National NMR Facility supported by FCT-Portugal (ROTEIRO/0031/2013–PINFRA/22161/2016, co-financed by FEDER through COMPETE 2020, POCI and PORL and FCT through PIDDAC). The 800 MHz spectrometer present in the "Manuel Rico" NMR laboratory (LMR-CSIC) is a node of the Spanish Large-Scale National Facility (ICTS R-LRB-MR).

CONFLICT OF INTEREST

The authors declare no conflict of interest.

DATA AVAILABILITY STATEMENT

The ^{1}H and ^{13}Cα NMR chemical shifts assignments of the polypeptide whose sequence corresponds to the FUS ZnF domain are available in the BMRB database under the access code 51614. All other data are contained within this article and in the Supporting Information.

ORCID

Javier Oroz https://orcid.org/0000-0003-2687-3013
Eurico J. Cabrita https://orcid.org/0000-0002-0720-2751

REFERENCES

Agashe VR, Udgaonkar JB. Thermodynamics of denaturation of Barstar: evidence for cold denaturation and evaluation of the interaction with guanidine hydrochloride. Biochemistry. 1995;34:3286–99.

Ahlers J, Adams EM, Bader V, Pezzotti S, Winklhofer KF, Tatzelt J, et al. The key role of solvent in condensation: mapping water in liquid-liquid phase-separated FUS. Biophys J. 2021;120:1266–75.

Ahlner A, Carlsson M, Jonsson B-H, Lundström P. PINT: a software for integration of peak volumes and extraction of relaxation rates. J Biomol NMR. 2013;56:191–202.

Al-Fageeh MB, Smales CM. Control and regulation of the cellular responses to cold shock: the responses in yeast and mammalian systems. Biochem J. 2006;397:247–59.

Annunziata O, Ogun O, Benedek GB. Observation of liquid-liquid phase separation for eye lens γS-crystallin. Proc Natl Acad Sci U S A. 2003;100:970–4.

Arakawa T, Timasheff SN. Stabilization of protein structure by sugars. Biochemistry. 1982;21:6536–44.

Arakawa T, Timasheff SN. The mechanism of action of Na glutamate, lysine HCl, and piperazine-N,N′-bis(2-ethanesulfonic acid) in the stabilization of tubulin and microtubule formation. J Biol Chem. 1984;259:4979–86.

Banani SF, Lee HO, Hyman AA, Rosen MK. Biomolecular condensates: organizers of cellular biochemistry. Nat Rev Mol Cell Biol. 2017;18:285–98.

Bentmann E, Neumann M, Tahirovic S, Rodde R, Dormann D, Haass C. Requirements for stress granule recruitment of fused in sarcoma (FUS) and TAR DNA-binding protein of 43 kDa (TDP-43). J Biol Chem. 2012;287:23079–94.

Boczek EE, Fürsch J, Niedermeier ML, Jawerth L, Jahnel M, Ruer-Gruß M, et al. HspB8 prevents aberrant phase transitions of FUS by chaperoning its folded RNA-binding domain. Elife. 2021;10:2021.439588.

Bosco DA, Lemay N, Ko HK, Zhou H, Burke C, Kwiatkowski TJ, et al. Mutant FUS proteins that cause amyotrophic lateral sclerosis incorporate into stress granules. Hum Mol Genet. 2010;19:4160–75.

Brangwynne CP. Phase transitions and size scaling of membrane-less organelles. J Cell Biol. 2013;203:875–81.

Brangwynne CP, Eckmann CR, Courson DS, Rybarska A, Hoege C, Gharakhani J, et al. Germline P granules are liquid droplets that localize by controlled dissolution/condensation. Science. 2009;324:1729–32.

Buchan JR. mRNP granules. RNA Biol. 2014;11:1019–30.

Buchan JR, Parker R. Eukaryotic stress granules: the ins and outs of translation. Mol Cell. 2009;36:932–41.

Burke KA, Janke AM, Rhine CL, Fawzi NL. Residue-by-residue view of in vitro FUS granules that bind the C-terminal domain of RNA polymerase II. Mol Cell. 2015;60:231–41.

Chen C, Ding X, Akram N, Xue S, Luo S-Z. Fused in sarcoma: properties, self-assembly and correlation with neurodegenerative diseases. Molecules. 2019;24:1622.

Courchaine EM, Lu A, Neugebauer KM. Droplet organelles? EMBO J. 2016;35:1603–12.

Da Vela S, Braun MK, Dörr A, Greco A, Möller J, Fu Z, et al. Kinetics of liquid-liquid phase separation in protein solutions exhibiting LCST phase behavior studied by time-resolved USAXS and VSANS. Soft Matter. 2016;12:9334–41.

Darling AL, Liu Y, Oldfield CJ, Uversky VN. Intrinsically disordered proteome of human membrane-less organelles. Proteomics. 2018;18:1700193.

Deng H, Gao K, Jankovic J. The role of FUS gene variants in neurodegenerative diseases. Nat Rev Neurol. 2014;10:337–48.

Dignon GL, Zheng W, Kim YC, Best RB, Mittal J. Sequence determinants of protein phase behavior from a coarse-grained model. PLoS Comput Biol. 2018;14:e1005941.

Dormann D, Rodde R, Edbauer D, Bentmann E, Fischer I, Hruscha A, et al. ALS-associated fused in sarcoma (FUS) mutations disrupt Transportin-mediated nuclear import. EMBO J. 2010;29:2841–57.

Elbaum-Garfinkle S, Kim Y, Szczepaniak K, Chen CC-H, Eckmann CR, Myong S, et al. The disordered P granule protein LAF-1 drives phase separation into droplets with tunable viscosity and dynamics. Proc Natl Acad Sci U S A. 2015;112:7189–94.

Gal J, Zhang J, Kwinter DM, Zhai J, Jia H, Jia J, et al. Nuclear localization sequence of FUS and induction of stress granules by ALS mutants. Neurobiol Aging. 2011;32:2323.e27–40.

Hamad N, Yoneda R, So M, Kurokawa R, Nagata T, Katahira M. Non-coding RNA suppresses FUS aggregation caused by mechanistic shear stress on pipetting in a sequence-dependent manner. Sci Rep. 2021;11:9523.

Hofmann S, Cherkasova V, Bankhead P, Bukau B, Stoecklin G. Translation suppression promotes stress granule formation and cell survival in response to cold shock. Mol Biol Cell. 2012;23:3786–800.

Jain S, Wheeler JR, Walters RW, Agrawal A, Barsic A, Parker R. ATPase-modulated stress granules contain a diverse proteome and substructure. Cell. 2016;164:487–98.

Jumper J, Evans R, Pritzel A, Green T, Figurnov M, Ronneberger O, et al. Highly accurate protein structure prediction with AlphaFold. Nature. 2021;596:583–9.

Kang J, Lim L, Lu Y, Song J. A unified mechanism for LLPS of ALS/FTLD-causing FUS as well as its modulation by ATP and oligonucleic acids. PLoS Biol. 2019;17:e3000327.

Kaur T, Alshareedah I, Wang W, Ngo J, Moosa M, Banerjee P. Molecular crowding tunes material states of ribonucleoprotein condensates. Biomolecules. 2019;9:71.

Keller R. Optimizing the process of nuclear magnetic resonance spectrum analysis and computer aided resonance assignment. Swiss Federal Institutes of Technology Zurich, 2004.

Kiwatkowsi T, Hosler BA, Cortelli P, Jong PJD, Yoshinaga Y, Haines JL. Mutations in the FUS/TLS gene on chromosome 16 cause familial amyotrophic lateral sclerosis. Science. 2009;547:1205–9.

Kluska K, Adamczyk J, Krężel A. Metal binding properties, stability and reactivity of zinc fingers. Coord Chem Rev. 2018;367:18–64.

Kroschwald S, Maharana S, Simon A. Hexanediol: a chemical probe to investigate the material properties of membrane-less compartments. Matters. 2017;3(5):e201702000010.

Li P, Banjade S, Cheng H-C, Kim S, Chen B, Guo L, et al. Phase transitions in the assembly of multivalent signalling proteins. Nature. 2012;483:336–40.

Li YR, King OD, Shorter J, Gitler AD. Stress granules as crucibles of ALS pathogenesis. J Cell Biol. 2013;201:361–72.

Lin Y, Protter DSW, Rosen MK, Parker R. Formation and maturation of phase-separated liquid droplets by RNA-binding proteins. Mol Cell. 2015;60:208–19.

Loughlin FE, Lukavsky PJ, Kazeeva T, Reber S, Hock EM, Colombo M, et al. The solution structure of FUS bound to RNA reveals a bipartite mode of RNA recognition with both sequence and shape specificity. Mol Cell. 2019;73:490–504.e6.

Martin SR, Esposito V, De Los RP, Pastore A, Temussi PA. Cold denaturation of yeast frataxin offers the clue to understand the effect of alcohols on protein stability. J Am Chem Soc. 2008;130:9963–70.

Mitrea DM, Kriwacki RW. Phase separation in biology; functional organization of a higher order. Cell Commun Signal. 2016;14:1.

Molliex A, Temirov J, Lee J, Coughlin M, Kanagaraj AP, Kim HJ, et al. Phase separation by low complexity domains promotes stress granule assembly and drives pathological fibrillization. Cell. 2015;163:123–33.

Murakami T, Qamar S, Lin JQ, Schierle GSK, Rees E, Miyashita A, et al. ALS/FTD mutation-induced phase transition of FUS liquid droplets and reversible hydrogels into irreversible hydrogels impairs RNP granule function. Neuron. 2015;88:678–90.

Murray DT, Kato M, Lin Y, Thurber KR, Hung I, McKnight SL, et al. Structure of FUS protein fibrils and its relevance to self-assembly and phase separation of low-complexity domains. Cell. 2017;171:615–627.e16.

Myers JK, Nick Pace C, Martin Scholtz J. Denaturant m values and heat capacity changes: relation to changes in accessible surface areas of protein unfolding. Protein Sci. 1995;4:2138–48.

Onuchic PL, Milin AN, Alshareedah I, Deniz AA, Banerjee PR. Divalent cations can control a switch-like behavior in heterotypic and homotypic RNA coacervates. Sci Rep. 2019;91(9):1–10.

Pace CN, Hermans J. The stability of globular protein. CRC Crit Rev Biochem. 1975;3:1–43.

Patel A, Lee HO, Jawerth L, Maharana S, Jahnel M, Hein MY, et al. A liquid-to-solid phase transition of the ALS protein FUS accelerated by disease mutation. Cell. 2015;162:1066–77.

Privalov PL. Cold denaturation of protein. Crit Rev Biochem Mol Biol. 1990;25:281–306.

Protter DSW, Parker R. Principles and properties of stress granules. Trends Cell Biol. 2016;26:668–79.

Psychogios N, Hau DD, Peng J, Guo AC, Mandal R, Bouatra S, et al. The human serum metabolome. PLoS One. 2011;6:e16957.

Rogelj B, Godin K, Shaw C, Ule J. The functions of glycine-rich regions in TDP-43, FUS and related RNA-binding proteins. RNA binding proteins. CRC Press; Austin, 2012. p. 59–74.

Rösner HI, Caldarini M, Prestel A, Vanoni MA, Broglia RA, Aliverti A, et al. Cold denaturation of the HIV-1 protease monomer. Biochemistry. 2017;56:1029–32.

Sama RRK, Ward CL, Bosco DA. Functions of FUS/TLS from DNA repair to stress response: implications for ALS. ASN Neuro. 2014;6:1–18.

Sanfelice D, Morandi E, Pastore A, Niccolai N, Temussi PA. Cold denaturation unveiled: molecular mechanism of the asymmetric unfolding of yeast Frataxin. ChemPhysChem. 2015;16:3599–602.

Scheper W, Hoozemans JJM. Endoplasmic reticulum protein quality control in neurodegenerative disease: the good, the bad and the therapy. Curr Med Chem. 2009;16:615–26.

Schindelin J, Arganda-Carreras I, Frise E, Kaynig V, Longair M, Pietzsch T, et al. Fiji: an open-source platform for biological-image analysis. Nat Methods. 2012;9:676–82.

Scimemi A, Beato M. Determining the neurotransmitter concentration profile at active synapses. Mol Neurobiol. 2009;40:289–306.

Shan B, McClendon S, Rospigliosi C, Eliezer D, Raleigh DP. The cold denatured state of the C-terminal domain of protein L9 is

compact and contains both native and non-native structure. J Am Chem Soc. 2010;132:4669–77.
Shin Y, Brangwynne CP. Liquid phase condensation in cell physiology and disease. Science. 2017;357:1–11.
Singh V, Xu L, Boyko S, Surewicz K, Surewicz WK. Zinc promotes liquid–liquid phase separation of tau protein. J Biol Chem. 2020;295:5850–6.
Sirabella R, Valsecchi V, Anzilotti S, Cuomo O, Vinciguerra A, Cepparulo P, et al. Ionic homeostasis maintenance in ALS: focus on new therapeutic targets. Front Neurosci. 2018;12:1–14.
Sirangelo I, Iannuzzi C. The role of metal binding in the amyotrophic lateral sclerosis-related aggregation of copper-zinc superoxide dismutase. Molecules. 2017;22:1429.
Sun Y, Chakrabartty A. Phase to phase with TDP-43. Biochemistry. 2017;56:809–23.
Szyperski T, Mills JL, Perl D, Balbach J. Combined NMR-observation of cold denaturation in supercooled water and heat denaturation enables accurate measurement of ΔCp of protein unfolding. Eur Biophys J. 2006;35:363–6.
Uversky VN, Kuznetsova IM, Turoverov KK, Zaslavsky B. Intrinsically disordered proteins as crucial constituents of cellular aqueous two phase systems and coacervates. FEBS Lett. 2015;589:15–22.
Varadi M, Anyango S, Deshpande M, Nair S, Natassia C, Yordanova G, et al. AlphaFold protein structure database: massively expanding the structural coverage of protein-sequence space with high-accuracy models. Nucleic Acids Res. 2022;50:D439–44.
Wang J, Choi JM, Holehouse AS, Lee HO, Zhang X, Jahnel M, et al. A molecular grammar governing the driving forces for phase separation of prion-like RNA binding proteins. Cell. 2018;174:688–699.e16.
Wong K-B, Freund SMV, Fersht AR. Cold denaturation of Barstar: ^{1}H, ^{15}N and ^{13}C NMR assignment and characterisation of residual structure. J Mol Biol. 1996;259:805–18.
Xiang S, Kato M, Wu LC, Lin Y, Ding M, Zhang Y, et al. The LC domain of hnRNPA2 adopts similar conformations in hydrogel polymers, liquid-like droplets, and nuclei. Cell. 2015;163:829–39.
Yan R, DeLos RP, Pastore A, Temussi PA. The cold denaturation of IscU highlights structure–function dualism in marginally stable proteins. Commun Chem. 2018;1:1–7.
Yang S, Warraich ST, Nicholson GA, Blair IP. Fused in sarcoma/translocated in liposarcoma: a multifunctional DNA/-RNA binding protein. Int J Biochem Cell Biol. 2010;42:1408–11.
Yoshizawa T, Ali R, Jiou J, Fung HYJ, Burke KA, Kim SJ, et al. Nuclear import receptor inhibits phase separation of FUS through binding to multiple sites. Cell. 2018;173:693.e1–693.e22.
Zhao Q, Guo Y, Ye T, Gasparrini A, Tong S, Overcenco A, et al. Global, regional, and national burden of mortality associated with non-optimal ambient temperatures from 2000 to 2019: a three-stage modelling study. Lancet Planet Health. 2021;5:e415–25.

SUPPORTING INFORMATION

Additional supporting information can be found online in the Supporting Information section at the end of this article.

How to cite this article: Félix SS, Laurents DV, Oroz J, Cabrita EJ. Fused in sarcoma undergoes cold denaturation: Implications for phase separation. Protein Science. 2023;32(1):e4521. https://doi.org/10.1002/pro.4521